A Numerical Study on Fracture-Plugging Behaviour of Granular Lost Circulation Materials
(Kajian Berangka Tingkah Laku Tampalan Retak Bahan Tak Teratur Bergranul)

GUI WANG* & XIAOLIN PU

ABSTRACT

A distinct element approach has been introduced for simulating the plugging performance of granular lost circulation materials (LCM) in a fracture. This approach solves the fully coupled fracture walls, fluid and particles system in an interactive environment. The effects of the particle shape, size distribution and concentration on the fracture-plugging performance of the granular LCM have been investigated using the three-dimensional particle flow code (PFC3D). The simulated results showed that the irregular granular LCM could plug a fracture width larger than the sieving granulation by single-particle bridging type. The particle size distribution (PSD) of LCM dominates the plugging depth and efficiency in a fracture and there exists an optimum concentration for maximum effect of LCM additives.

Keywords: Fracture; lost circulation material; numerical simulation; plugging

ABSTRAK

Pendekatan elemen berbeza telah diperkenalkan bagi mensimulasi prestasi tampalan bahan tak teratur (LCM) bergranul dalam retakan. Pendekatan ini menyelesaikan masalah dinding retak berganding penuh, bendalir serta sistem zarah dalam persekitaran interaktif. Kesan bentuk zarah, pengagihan saiz dan kepekatan terhadap prestasi tampalan retak LCM bergranul telah dikaji menggunakan kod aliran zarah tiga dimensi (PFC3D). Keputusan simulasi menunjukkan bahawa LCM bergranul yang tidak sekata boleh menampal retak yang lebih besar daripada penyaringan penggranulan mengikut jenis penyambung satu zarah. Taburan saiz zarah (PSD) daripada LCM menguasai kedalaman tampalan serta kecekapan dalam retak dan wujud kepekatan optimum untuk kesan maksimum aditif LCM.

Kata kunci: Bahan tak teratur; retak; simulasi berangka; tampalan

INTRODUCTION

Lost circulation has always been a serious and expensive problem when drilling through fractured formations (George & Scott 1951). A common cure of this problem is the introduction of granular lost circulation materials (LCM) into the drilling fluid system. Granular LCM are then carried and forced into fractures by drilling fluid under differential pressure. Proper LCM may establish an efficient bridge plug inside fracture formations (Dick et al. 2000; Kaageson-Loe et al. 2009; Whitfill & Hemphill 2003). A right and clear understanding of the fracture-plugging performance of granular LCM is essential to design the LCM and the treatment for circulation losses into fractured formations with a higher success rate.

In the past, various researchers have carried out a series of theoretical analyses and experiments to investigate the fracture-plugging performance of granular LCM and many valuable viewpoints have been obtained from these existing researches (Dick et al. 2000; Fathi et al. 2004; Gatlin & Nemir 1961; Moazzeni. 2012; Nayberg 1987; Pilehvari & Venkata 2002; Whitfill & Hemphill 2003).

However, due to the absence of analytical solution and the difficulties of monitoring the full complicated movement and interaction process, the cognizance of the fracture-plugging performance of granular LCM remains limited. In order to make clear plugging behaviour of granular LCM in fractured formations, numerical simulation method ought to be considered. However, because of the difficulties encountered to this kind of simulation, there hardly exists a numerical attempt for this intricate problem yet.

Amongst all numerical approaches, distinct element method (DEM) may handle such a complicated process as it has the capability of modelling the movement and interaction of discrete particles (Fortin et al. 2005). In order to facilitate the simulation of the complex plugging process of granular LCM in a vertical fracture, the three-dimensional particle flow code (PFC3D), a numerical simulator developed by Cundall and Strack (1979), was adopted directly in the present work. The effects of particle shape, size distribution and concentration on the fracture-plugging performance were analysized according to the simulation results.

MODEL DESCRIPTION

PFC3D PROGRAM

PFC3D is a program used to perform research into the element behaviour of granular material. It models the movement and interaction of spherical particles by the distinct element method. It is also possible to create particles of arbitrary shape by attaching two or more particles together, such that each group of particles acts as an autonomous object (Cundall & Stack 1979; Itasca 2003).

The calculations performed in PFC3D alternate between the application of Newton's second law to the particles and a force-displacement law at the contacts (Itasca 2003). Contacts, which may exist between two balls or between a ball and a wall, are formed and broken automatically during the course of simulation. The calculation cycle is shown in Figure 1.

update particle + wall positions and set of contacts

Law of Motion
• Resultant force + moment

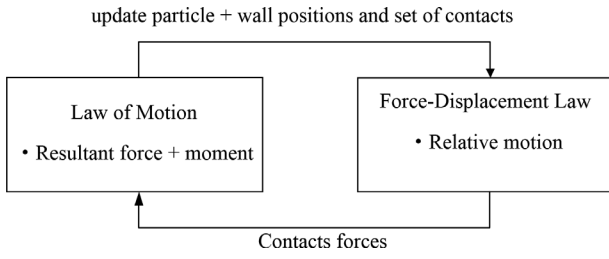Force-Displacement Law
• Relative motion

Contacts forces

FIGURE 1. Calculation cycle in PFC3D

At the start of each timestep, the set of contacts is updated from the known particle and wall positions. The force-displacement law is then applied to each contact to update the contact forces based on the relative motion between the two entities at the contact constitutive model. Next, Newton's second law is applied to each particle to update its velocity and position based on the resultant force and moment arising from the contact forces and anybody forces acting on the particle. Also, the wall positions are updated based on the specified wall velocities.

BASIC EQUATIONS

For particle i, as shown in Figure 2, the translational and rotational motion can, respectively, be described by:

$$\mathbf{F}_i = m_i \frac{d\mathbf{V}_i}{dt} = \sum \left(\mathbf{F}_{ij}^n + \mathbf{F}_{ij}^s \right) + \mathbf{F}_{\nabla p,i} + \mathbf{F}_{drag,i} + \mathbf{F}_{buoy,i} + m_i \mathbf{g}, \quad (1)$$

and

$$\mathbf{T}_i = \mathbf{I}_i \frac{d\boldsymbol{\omega}_i}{dt} = \sum_j \left(\mathbf{R}_{ij} \times \mathbf{F}_{ij}^s - \mu_r R_i \left| F_{ij}^n \right| \hat{\omega}_i \right), \quad (2)$$

where $\mathbf{F}_i$ and $\mathbf{T}_i$ are the total forces and torques acting on the particle, m_i, $\mathbf{v}_i$, $\boldsymbol{\omega}_i$, and $\boldsymbol{I}_i$ are, respectively, the mass, transitional velocity, angular velocity and moment of
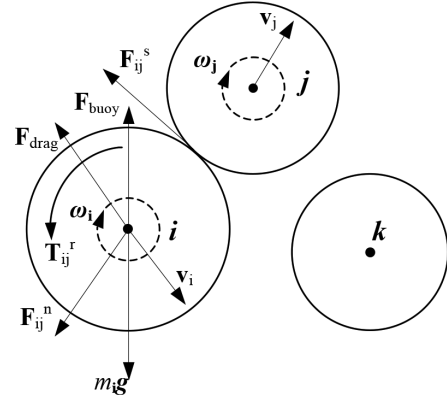
FIGURE 2. Schematic illustrations of the forces exerting on particle i

inertial of particle i; $\mathbf{g}$ is the gravitational acceleration; $\mathbf{R}_{ij}$ is the vector pointing from the center of particle i to the contact point with particle j; μ_r is the rolling friction coefficient and $\hat{\omega}_i = \omega_i / |\omega_i|$ and $\mathbf{F}_{ij}^n$ and $\mathbf{F}_{ij}^s$ are the normal and tangential contact forces, respectively, which can be given as:

$$\mathbf{F}_{ij}^n = \left[\frac{2}{3} E\sqrt{\bar{R}}\xi_n^{\frac{3}{2}} - \gamma_n E\sqrt{\bar{R}}\sqrt{\xi_n} \left(\mathbf{V}_{ij} \cdot \hat{\mathbf{n}}_{ij} \right) \right] \hat{\mathbf{n}}_{ij}. \quad (3)$$

$$F_{ij}^s = \mu_r |F_n| \left[1 - \left(1 - \min\left(\xi_s, \xi_{s,max} \right) / \xi_{s,max} \right)^{3/2} \right] \hat{\mathbf{n}}_{ij}, \quad (4)$$

where $\bar{R} = R_i R_j / (R_i + R_j)$, $E = Y/(1 - \tilde{\sigma}^2)$ $\boldsymbol{R}_i$ and $\boldsymbol{R}_j$ are the radii of particles i and j, respectively; Y and $\tilde{\sigma}$ are, respectively, Young's modulus and Poisson's ratio. $\hat{\mathbf{n}}_{ij}$ is a unit vector running from the center of particle j to the particle i. μ_s and γ_n are the sliding friction and the normal damping coefficient, respectively. $\xi_{s,max}$ and ξ_s are, respectively, the maximum and total tangential displacements of particles during contact.

In order to extend the DEM model to the particle-fluid system, the interactions between fluid and particles should be incorporated. Although there are a range of forces in such system, not all are important in a particular application. In the present work, three forces are considered, i.e. the buoyancy force, pressure gradient force and drag forces, respectively, given by:

$$\mathbf{F}_{buoy,i} = -\frac{4\pi}{3} R_i^3 \rho_f \mathbf{g}. \quad (5)$$

$$\mathbf{F}_{\nabla p,i} = \frac{4\pi}{3} R_i^3 \nabla p. \quad (6)$$

$$\mathbf{F}_{drag,i} = \mathbf{f}_{f0,i} \varepsilon_i^{-x}, \quad (7)$$

where,

$$\mathbf{f}_{f0,i} = 0.5 C_{d0,i} \rho_f \pi R_i^2 \varepsilon_i^2 \left| \mathbf{v}_f - \mathbf{v}_i \right| (\mathbf{v}_f - \mathbf{v}_i), \quad C_{d0,i} = (0.63 + \frac{4.8}{Re_i^{0.5}})^2,$$

$$Re = \frac{2\rho_f R_i \varepsilon_i \left| \mathbf{v}_f - \mathbf{v}_i \right|}{\mu_f} \text{ and } \chi = 3.7 - 0.65 \exp\left[-\frac{(1.5 - \log_{10} Re)^2}{2} \right].$$

p,$\mathbf{v}_f$, ρ_f and μ_f are, respectively, the fluid pressure, velocity, density and viscosity.

SIMULATION PARAMETERS

In this work, vertical fracture is considered to represent the majority of fractures encountered (George & Scott 1951; Kaageson-Loe et al. 2009). The simulated fracture consists of two vertical jagged walls with height H_f, length L_f, inlet width W_i and outlet width W_o. The detail geometrical conditions are listed in Table 1.

The particulate-treated drilling fluid flow is assumed to be one-dimensional along the fracture length direction with the base fluid viscosity μ_f and density ρ_f at the differential pressure Δp. The fixed coarse-grid fluid scheme has been used to implement the particle-fluid coupling in simulation (Apostolou & Hrymak 2008).

Table 1 gives the material properties used in the simulation, which are based on the properties of calcium carbonate particles. This work considers the irregularity of LCM particle, because many granular LCM, such as nut shells and calcium carbonate particles, are always rigid particles with shapes of angular rather than circular or spherical (Pilehvari & Venkata 2002). In this study, the granular particles larger than 0.45 mm are represented by irregular particles of equal volumes, while the other granules were represented by spherical particles. The bridge particles with irregular shape are modeled using the so-called overlapping discrete element cluster (ODEC) algorithm, as shown in Figures 3 and 4. In ODEC method, the representative assemblies of angular particles are generated by inscribing a number of overlapping spherical balls within the particle outline (Fortin et al. 2005; Garicia et al. 2009; Lu & McDowell 2006).

TABLE 1. Parameters in the simulation

| Parameter	Value	Parameter	Value
Fracture height, H_f	10 mm	Particle density, ρ_p	2.7 g·cm^{-3}
Fracture length, L_f	150 mm	Particle size, d	0.25-2.0 mm
Fracture inlet width, W_i	2.0 mm	Young's modulus of particles, Y	45×10^9 Pa
Fracture outlet width, W_o	1.0 mm	Poisson's ratio of particles, $\tilde{\sigma}$	0.25
Fluid density, ρ_f	1.05 g·cm^{-3}	Damping coefficient, γ_n	5×10^{-5}
Fluid viscosity, μ_f	100 mPa·s	Sliding friction coefficient, μ_s	0.3
Differential pressure, Δp	6×10^6 Pa	Rolling friction coefficient, μ_r	0.01
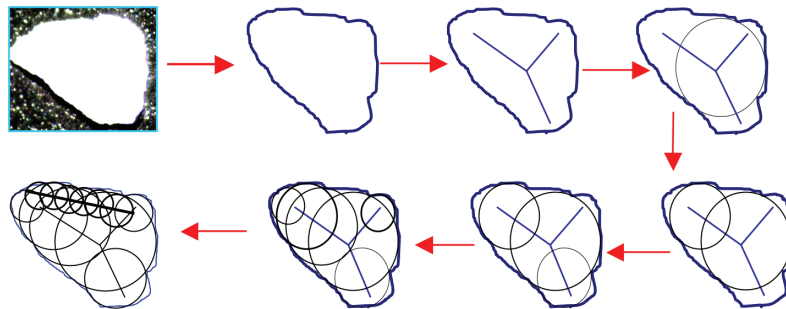
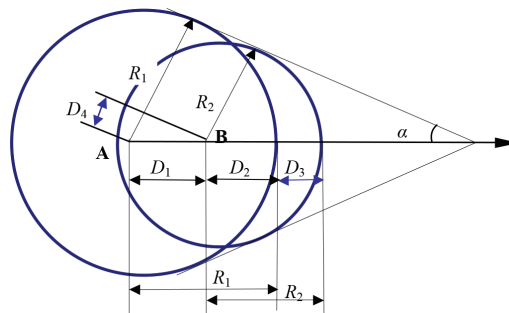FIGURE 3. Schematic diagram of ODEC procedure

FIGURE 4. Definition of clump geometry

RESULTS AND DISCUSSION

PARTICLE SHAPE EFFECT

As the manner of passing through a sieve mesh is quite different between irregular particles and spherical particles, the size of irregular granular LCM in certain direction often grows up than the sieve mesh side (Pilehvari & Venkata 2002; Whitfill & Hemphill 2003).

In order to investigate the effect of particle shape on the fracture-plugging performance of granular LCM, this work simulated the fracture-plugging performances of nonspherical particles with equal volume to the spherical particles, which have the same equivalent diameter of 2 mm. The simulated outcomes of spherical and nonspherical particles of the equal volume are shown in Figure 5.

As can be seen from Figure 5, when the equivalent particle diameter equals to the fracture opening width, the spherical particles can plug inside fracture near the mouth, whereas the nonspherical particle of an equal volume can only block outside. The latter case is an unexpected plugging type in drilling industry, because the LCM will become dislodged easily as a result of drilling stem rotating or colliding as well as drilling fluid flushing. Hence the irregularity of particle should be taken into account to avoid plugging outside fracture. Moreover, it was observed at a particle scale during the simulation process that the granular LCM particle blocked fracture in the type of single-particle rather than multiple-particle bridging, which leads us to further believe that the granular LCM particles plug the fracture width larger than its sieving grain size due to the irregularity of shape.

PARTICLE SIZE DISTRIBUTION EFFECT

Particle size distribution (PSD) is always thought to be the most important factor impacting the plugging performance of granular LCM in fractured formations (Dick et al. 2000; Gatlin & Nemir 1961; Loeppke et al. 1990; Moazzeni et al. 2012; Pilehvari & Venkata 2002). For ease of presentation and study, the list of grain size grade for granular LCM is shown in Table 2.

In this study, the granular particles larger than 0.45 mm (40 mesh) were represented by irregular particles of equal volumes, while the other granules were represented by spherical particles. The simulation results for the four selected typical PSD of LCM are shown in Table 3 and Figure 6.
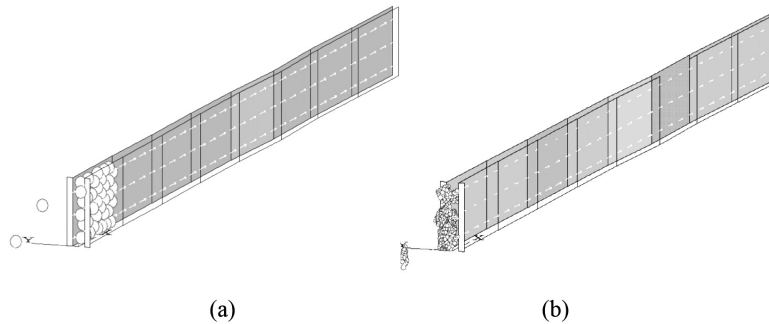

(a)   (b)

FIGURE 5. Snapshots showing the fracture-plugging performances of spherical and nonspherical particles of the equal volume

TABLE 2. Grain size grade for granular LCM

Grade	A	B	C			
			C1	C2	C3	C4
Size (mm)	0.25-0.45	0.45-0.9	0.9-1.2	1.2-1.4	1.4-1.7	1.7-2.0

TABLE 3. Simulation results for different PSD of the same concentration

Case	Formulation of LCM	d_{10} (mm)	d_{50} (mm)	d_{90} (mm)	Plugging depth (mm)	Time spent (10^{-3}s)
1	6% A+1% B	0.15	0.45	0.8	/	/
2	1.5% A+4% B+1.5% C1	0.25	0.7	1.05	130-150	30
3	1.5% A+1.5% B+3% C1+1% C2	0.25	1.0	1.25	80-100	23
4	1% A+1% B+1% C1+1% C2+2% C3+1% C4	0.25	1.3	1.75	0	13

From the simulation results, it can be clearly seen that both the plugging depth and time spent before plugging are related closely to the particle size distribution of LCM. The larger the value of d_{50} and d_{90}, the shallower the plugging depth and the shorter time before plugging. However, too large d_{50} and d_{90} values of LCM are harmful to plugging inside fractures, because too coarse particles in LCM cannot enter fracture effectively and in consequence plug outside the fracture as case 4 shown in Figure 6(d). Although the calculation time is about half an hour, the actual physical time spent before plugging needs only several milliseconds. The milliseconds time, decreased with the d_{50} and d_{90} values of LCM, indicated that the fracture plugging process was instantaneous. Therefore, appropriate particle size distribution, especially the values of d_{50} and d_{90}, is critical to plugging inside the fractures effectively and efficiently.

PARTICLE CONCENTRATION EFFECT

Besides particle shape and size distribution, the particle concentration also has significant impact on the plugging performance of granular LCM in a fracture (Moazzeni et al. 2012; Nayberg 1987). In order to investigate the effect of particle concentration, this study simulated the fracture-plugging performance at different concentration of 3.5, 7, 14 and 21% by weight, respectively. The simulation results showed that the effect of particle concentration on the plugging depth is negligible, whereas the effect of particle concentration on the time need to plug is significant. The particle concentration effect on time spent before plugging is shown in Figure 7.

From Figure 7, a nonlinear relation is obviously seen to prevail between the particle concentration and the time spent before plugging. The time spent before plugging decreases sharply until a certain concentration value, which may be called the *optimum concentration*. Many other researchers have also reported that there exists an optimum particle concentration for maximum effect of the LCM additive through their experiments (Dick et al. 2000; Moazzeni et al. 2012), which leads us to believe the accuracy of simulation result is high enough. It is concluded that the plugging efficiency can be improved
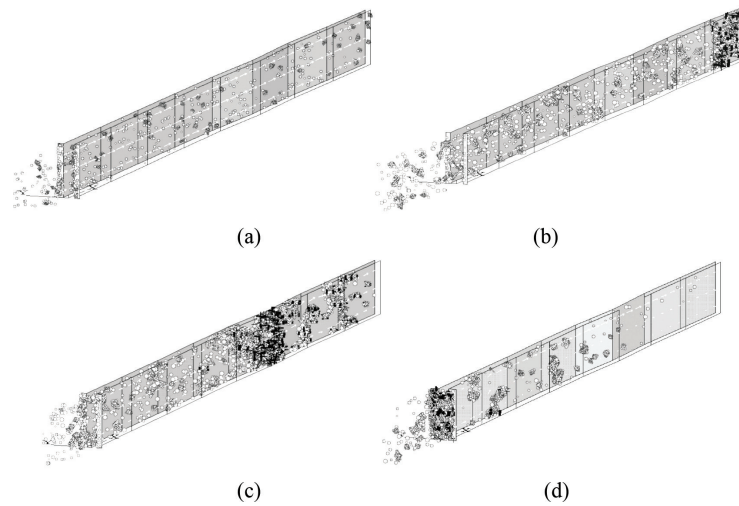

FIGURE 6. Snapshots showing the plugging outcomes of different PSD: (a) not plug (case 1),
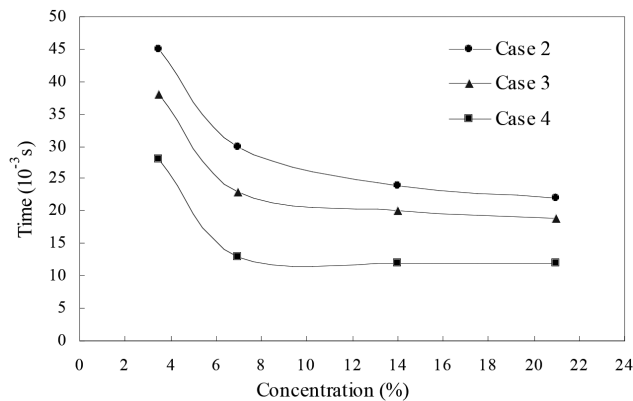(b) plug at tip (case 2), (c) plug at middle part (case 3) and (d) plug outside (case 4)

FIGURE 7. The time spent before plugging for different particle concentrations

812

significantly by increasing the concentration up to the optimum value and any increase of LCM concentration over the optimum concentration will not improve its plugging performance significantly.

CONCLUSION

Due to the irregularity of particle, granular LCM are able to plug a fracture width larger than the sieving granulation by the type of single-particle bridging. The D_{50} and D_{90} values of the LCM's particle size distribution dominate the plugging depth and efficiency in fractured formations. There exists an optimum concentration for maximum effect of granular LCM.

REFERENCES

Apostolou, K. & Hrymak, A.N. 2008. Discrete element simulation of liquid-particle flows. *Computers & Chemical Engineering* 4-5: 841-856.

Cundall, P.A. & Strack, O.D. 1979. A discrete numerical model for granular assembles. *Geotechanique* 1: 47-65.

Dick, M.A., Heinz, T.J., Svoboda, C.F. & Aston, M. 2000. Optimizing the selection of bridging particles for reservoir drilling fluids. SPE Paper 58793. *SPE International Symposium on Formation Damage Control*, Lafayette, Louisiana. February 23-24.

Fathi, B., Basma, Y., Hamoud, A.H., Ali, B., Tayfun, B. & Peter, D.M. 2004. A comparative study of lost circulation materials. *Energy Sources* 26: 1043-1051.

Fortin, J., Millet, O. & Saxcé, G.D. 2005. Numerical simulation of granular materials by an improved discrete element method. *International Journal for Numerical Methods in Engineering* 62: 639-663.

George, C.H. & Scott, P.P. 1951. An analysis and the control of lost circulation. *Journal of Petroleum Technology* 3(6): 171-182.

Gatlin, C. & Nemir, C.E. 1961. Some effects of size distribution on particle bridging in lost circulation and filtration tests. *Journal of Petroleum Technology* 6: 575-578.

Garcia, X., Latham, J.P., Xiang, J. & Harrison, J.P. 2009. A clustered overlapping sphere algorithm to represent real particles in discrete element modeling. *Geotechnique* 9: 779-784.

Itasca Consulting Group, Inc. 2003. PFC3D (particle flow code in 3 dimension) version 3.1. Itasca Consulting Group, Inc.

Kaageson-Loe, N.M., Sanders, M.W., Growcock, F., Taugbol, K., Horsrud, P., Singelstad, A.N. & Omland, T.H. 2009. Particulate-based loss-prevention material - The secrets of fracture-sealing revealed. *SPE Drilling & Completion* 24(4): 581-589.

Loeppke, G.E., Glowka, D.A. & Wright, E.K. 1990. Design and evaluation of lost-circulation materials for severe environments. *Journal of Petroleum Technology* 3: 328-337.

Lu, M. & McDowell, G.R. 2006. The importance of modeling ballast particle shape in the discrete element method. *Granular Matter*. 1: 69-80.

Moazzeni, A., Nabaei, M. & Kharrat, R. 2012. A breakthrough in controlling lost circulation in a pay zone by optimizing the particle size distribution of shellfish and limestone chips. *Petroleum Science and Technology* 3: 290-306.

Nayberg, T.M. 1987. Laboratory study of lost circulation materials for use in both oil-based and water-based drilling muds. *SPE Drilling Engineering* 3: 229-236.

Pilehvari, A.A. & Venkata, R.N. 2002. Effect of material type and size distribution on performance of loss/seepage control material. SPE Paper 73791. *International Symposium and Exhibition on Formation Damage Control*, Lafayette, Louisiana. February 20-21.

Whitfill, D.L. & Hemphill, T. 2003. All lost-circulation materials and systems are not created equal. SPE Paper 84319. *SPE Annual Technical Conference and Exhibition*, Denver, Colorado. October 5-8.

State Key Laboratory of Oil
& Gas Reservoir Geology and Exploitation
Southwest Petroleum University
Xindu, Chendu, Sichuan
P. R. China

*Corresponding author; email: wanggui@126.com